Impedance and power fluctuations in linear chains of coupled wave chaotic cavities

Gabriele Gradoni,* Thomas M. Antonsen, Jr., and Edward Ott
Institute for Research in Electronics and Applied Physics, University of Maryland, College Park, 20742 Maryland, USA
(Received 7 February 2012; revised manuscript received 16 July 2012; published 5 October 2012)

The flow of electromagnetic wave energy through a chain of coupled cavities is considered. The cavities are assumed to be of sufficiently irregular shape that their eigenmodes are described by random matrix theory. The cavities are coupled by electrically short single mode transmission lines. Approximate expressions for the power coupled into successive cavities are derived, and the predictions are compared with Monte Carlo simulations. The analytic formulas separate into a product of factors. Consequently, the distribution of power in the last cavity of a very long chain approaches lognormal. For lossless cavities, signatures of Anderson localization, similar to those of the conductances of quantum wires, are observed.

DOI: 10.1103/PhysRevE.86.046204 PACS number(s): 05.45.Mt, 03.50.De, 42.25.Bs, 24.60.−k

I. INTRODUCTION

Over the past few decades, there has been considerable progress in understanding and characterizing complex wave systems. In particular, the statistical aspects of wave scattering in diverse areas, such as acoustics [1], mesoscopic electron physics [2], nuclear physics [3], and electromagnetics [4] have been studied. The successful underlying approach to understanding these systems is based on the application of random matrix theory (RMT) [5–7]. In this approach, system-specific information about the wave scattering system is combined with a statistical model based on the eigenfunctions and eigenvalues of a random matrix from a well-defined ensemble to construct a model for wave transport through the system [8,9]. This statistical approach is used in lieu of a first principles solution of the relevant wave equation. Such a first principles solution is often not practical. It requires an accurate description of the scattering geometry, which may not be known. At the same time, the solutions are extremely sensitive to frequency and, thus, must be repeated if the source wave form is changed. Finally, the first principles solutions can be computationally demanding particularly in the limit where the system size is much bigger than a wavelength.

Whereas, much work has focused on the scattering in relatively simple systems that can be characterized as an enclosed region with ports for the ingress and egress of waves, less work has been devoted to the study of combinations of such systems in which waves move from one enclosed region to another. Our paper here is motivated by the desire to understand the distribution of electromagnetic radiation from one enclosed region or cavity to another through ports that can be characterized by a single pair of waves. Our focus will be on the statistics of the electromagnetic fields in a chain of coupled cavities.

An important assumption that we make is that the coupling between two contiguous cavities takes place through a small port, and electromagnetic energy flows in a single propagation mode from one cavity to another through a short cable, whose electrical length is neglected and can be modeled as a direct connection. This allows us to model the cavities using impedance matrices in which the connection between two cavities is treated as a junction of a port of one cavity with that of another. This is in distinction to an earlier paper on chains of coupled structures that are relatively open [10]. Recently, a different investigation [11] focused on coupling between quantum dots. The authors studied an Aharonov-Bohm ring containing two cavities, a regular and a chaotic one. Conductance oscillations and related distributions have been derived in closed form, and the role of the RMT ensemble was discussed. The coupling of reverberant environments through apertures and loading materials has also been addressed [12,13]. A model for frequency [12] and time [13] domain cumulative buildup of electromagnetic energy in coupled (reverberant) spaces was derived by using conservation of average energy and a model developed in the framework of acoustic theory. Our model is distinct from this paper in that it allows for interference effects that are not captured based on consideration of energy conservation. Furthermore, we determine the circumstances under which this interference is important.

In our papers, each cavity was assumed to be governed by the random coupling model [14–17] in which the elements of the impedance matrix for the cavity were expressed in terms of the radiation impedances of the ports, and eigenfunctions and eigenvalues of a random matrix drawn from the Gaussian orthogonal ensemble (GOE) [7]. Joint application of electrical network theory and the random coupling model leads to a compact expression for the voltages appearing at the inputs of cavities in the chain in the form of recursion relations. In the high-loss limit, it is possible to evaluate these recursion relations, and the expression for the power delivered to each cavity can be written as a product of factors. The factors separate into two groups: system-specific factors describing the interconnection of the ports and the loss factors of the cavities, and universal statistical factors that describe the fluctuations. As a consequence, the distribution function (DF) of the coupled power is well approximated by the DF of the product of N identical random variables where N is the cavity number. Furthermore, the distribution function for the power coupled to the Nth cavity (after appropriate normalization by nonstatistical quantities) becomes universal in that it depends only on the number of cavities.

In the absence of losses, the coupled power ratio can be expressed in terms of a product of N random 2×2 matrices with a unit determinant in analogy to the Anderson localization

*Corresponding author.

problem. In this case, the distribution function of the power ratio for a chain of N cavities, while approaching lognormal, depends in a complicated way on system-specific parameters. We note that, for parameters considered here, the power ratio DF in the lossless case approaches lognormal more rapidly with N than it does in the high-loss case.

The organization of this paper is as follows. In Sec. II, we consider the simple case of two coupled cavities and derive expressions for the transimpedance and the coupled power. These formulas are then compared with results from Monte Carlo simulations. In Sec. III, we generalize the results of Sec. II for chains of cavities of arbitrary length. Monte Carlo simulations of these cases are also presented. In this section, we discuss the localized regime for a chain of lossless cavities. In Sec. IV, we show the structure impedance convergence in terms of the inverse of the localization length. Finally, in Sec. V, we discuss the application of our results to more general configurations and give our conclusions.

II. RANDOM COUPLING MODEL FOR TWO CONNECTED CAVITIES

We first consider the case of two coupled cavities as illustrated schematically in Fig. 1. Cavity 1 has two ports: It is excited by a source at port 1, and it is connected at port 2 through a transmission line to cavity 2. Each cavity is described by an impedance matrix that relates the voltages and currents at the ports $\underline{V} = \underline{\underline{Z}} \cdot \underline{I}$. For the case of cavity 1, the impedance matrix is 2×2, whereas, for cavity 2, the impedance matrix is a scalar. The two cavities are connected by a transmission line of characteristic impedance Z_0, and transit time τ. Given a source excitation at the first cavity, we wish to find the level of signal at the input of cavity 2. From this, we can determine the amount of power that is coupled into cavity 2 and from this, the level of signal within cavity 2.

The treatment of the ports as simple terminals characterized by a single voltage and current assumes that the ports are smaller than a wavelength of the radiation inside the cavity. If this is not the case, then each port must be characterized by a set of voltages and currents. These voltages and currents will be related in a way that depends explicitly on the geometry of the port. This requires the addition of a certain amount of system-specific information. In order to keep the description simple, we will focus on the case of small ports.

All the details of the interior of the cavities are contained in the impedance matrices. In the limit in which the cavities

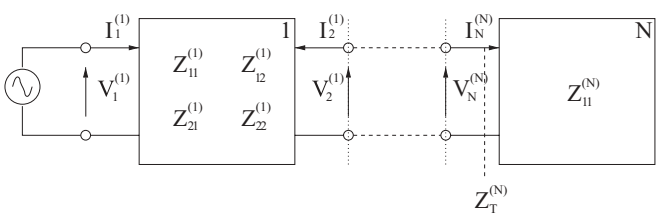

FIG. 1. Network model of a chain of coupled cavities: The first cavity is excited by a source, whereas, the power leaking out excites the subsequent ones. The port approximation takes place when the current injection and leakage are spatially localized, hence the electrical network theory can be used.

are large compared with a wavelength, the values of the elements of the impedance matrices are sensitive functions of both the frequency and the geometric properties of the cavity. In this limit, the cavity impedance can be treated as a statistical quantity whose properties are predicted by RMT [7]. Specifically, in the limit in which wave energy passes indirectly from one port to another by many reflections in the interior of the cavity, the impedance matrix has the following form [15]:

$$\underline{\underline{Z}} = j\underline{\underline{X}}_{\rm rad} + \underline{\underline{R}}_{\rm rad}^{1/2}\,\underline{\underline{\xi}}\,\underline{\underline{R}}_{\rm rad}^{1/2}, \tag{1}$$

where

$$\underline{\underline{Z}}_{\rm rad} = j\underline{\underline{X}}_{\rm rad} + \underline{\underline{R}}_{\rm rad} \tag{2}$$

is a diagonal matrix whose elements are the radiation impedances of the ports looking into the cavity in the case in which no radiation returns to the port, for example, if the walls of the cavity are absorbing. In Eqs. (1) and (2), $\underline{\underline{R}}_{\rm rad} = {\rm Re}(\underline{\underline{Z}}_{\rm rad})$ stands for the radiation resistance, whereas, $\underline{\underline{X}}_{\rm rad} = {\rm Im}(\underline{\underline{Z}}_{\rm rad})$ stands for the radiation reactance. Statistical fluctuations in impedance that account for multiple reflections of wave energy in the cavity are described by the complex matrix $\underline{\underline{\xi}}$ whose elements are determined by RMT. An algorithm for generating values for $\underline{\underline{\xi}}$ will be given subsequently. The statistical properties of $\underline{\underline{\xi}}$ depend on a single parameter that characterizes the losses in the cavity. Expressions (1) and (2) have been tested by comparison with measurement and computation in a variety of contexts [16,17]. Furthermore, (1) has been generalized to account for the direct propagation of wave energy from one port to another [18,19]. Use of the generalized formula requires additional information about the cavity, and we defer consideration of this point.

The simplest way to generate sample values for the matrix $\underline{\underline{\xi}}$ is to use a Monte Carlo method. Specifically, values for the element $\xi_{\rm pl}$ can be generated by computing the sum,

$$\xi_{\rm pl} = \frac{i}{\pi}\sum_m \frac{\Delta k^2 w_{pm} w_{lm}}{k^2(1 - j/Q) - k_m^2}, \tag{3}$$

where m stands for the "chaotic mode" index, $j = \sqrt{-1}$ represents the imaginary unit, $j = -i$, and w_{pm} and w_{lm} are independent and identically distributed Gaussian random variables with zero mean and unit variance. The quantities k_m^2 mimic the resonant frequencies of the cavity $\omega_m = k_m c$, $\omega = kc$ is the excitation frequency, and Q is the typical (average) quality factor of the cavity (not including the effect of the two ports). The mean spacing in resonant frequencies in the range of ω determines Δk^2. Specifically, $\Delta k^2 = \langle \omega_{m+1}^2 - \omega_m^2 \rangle / c^2$ where the angular brackets indicate an average over resonant frequencies in the range of ω. For electromagnetic modes (two polarizations) in a cavity of volume V, Weyl's formula for the number of modes with a frequency less than ω, $M(\omega) = (\omega/c)^3 V/(3\pi^2)$, predicts the value $\Delta k^2 = 2\pi^2 c/(\omega V)$.

The quantities k_m^2 are determined by the eigenvalues of a large $M \times M$ random matrix ($M \gg 1$) selected from the GOE. These eigenvalues are distributed roughly between $\pm M^{1/2}$ with a mean spacing that scales as $M^{-1/2}$ around zero eigenvalues. The eigenvalues of this GOE matrix [7] are then shifted and are scaled in value, becoming the k_m^2 values. Shifting and scaling is performed in such a way that roughly

equal numbers of eigenvalues fall above and below k^2, and such that the mean spacing of k_m^2 values near k^2 is Δk^2. With this prescriptions for defining the elements of $\underline{\underline{\xi}}$, one can show that $\langle \underline{\underline{\xi}} \rangle = \underline{\underline{1}}$, where $\underline{\underline{1}}$ is the identity matrix and the angular brackets $\langle \cdot \rangle$ now indicate an average over an ensemble of realizations of Eq. (3). From this, it follows that the average cavity impedance is the radiation impedance,

$$\langle \underline{\underline{Z}} \rangle = \underline{\underline{Z}}_{\rm rad}. \tag{4}$$

The probability distribution functions for the elements of $\underline{\underline{\xi}}$ depend only on the single loss parameter [9,14–17],

$$\alpha = \frac{k^2}{(Q\ \Delta k^2)}, \tag{5}$$

which measures the Q width of a cavity resonance in terms of the average spacing between cavity resonances. Here, the losses are assumed to be internal to the cavity and are not losses associated with coupling to either of the two ports. A limit that we treat analytically is the case of high loss, $\alpha \gg 1$. In this case,

$$\underline{\underline{\xi}} = \underline{\underline{1}} + \delta\underline{\underline{\xi}}, \tag{6}$$

where the individual elements $\delta\xi_{\rm pl}$ are small complex zero mean Gaussian random variables with independent real and imaginary parts. The variance in the real and imaginary parts of the off-diagonal elements is $(2\pi\alpha)^{-1}$, and the variance in the real and imaginary parts of the diagonal elements is $(\pi\alpha)^{-1}$ [15]. Thus, the magnitude squared of each element is given by an exponential distribution,

$$P(|\delta\xi_{\rm pl}|^2) = \sigma\ \exp(-\sigma|\delta\xi_{\rm pl}|^2), \tag{7}$$

where $\sigma = (2\pi\alpha)^{-1}$ for off-diagonal elements and $\sigma = (\pi\alpha)^{-1}$ for diagonal elements. We note that, in the limit of large losses, $\alpha \to \infty$, $\underline{\underline{Z}} \to \underline{\underline{Z}}_{\rm rad}$.

We now analyze the configuration shown in Fig. 1 for $N = 2$. The voltages and currents for cavity 1 are written explicitly,

$$V_1^{(1)} = Z_{11}^{(1)} I_1^{(1)} + Z_{12}^{(1)} I_2^{(1)}, \tag{8a}$$

$$V_2^{(1)} = Z_{21}^{(1)} I_1^{(1)} + Z_{22}^{(1)} I_2^{(1)}, \tag{8b}$$

where the subscripts label ports (p and l), and the superscripts label cavity number. For cavity 2, we have a scalar equation,

$$V_1^{(2)} = Z_{11}^{(2)} I_1^{(2)}. \tag{9}$$

We neglect, for the moment, the time delay in the transmission line connecting cavities 1 and 2, in which case, we can equate the voltages at port 2 of cavity 1 and port 1 of cavity 2, and we relate the currents entering the two connected ports,

$$V_2^{(1)} = V_1^{(2)}, \tag{10a}$$

$$I_1^{(2)} = -I_2^{(1)}. \tag{10b}$$

Solving Eqs. (8)–(10), we can express the voltage at the input of cavity 2 for the current at the input of cavity 1 with cavity 2 as a load,

$$V_2^{(1)} = Z_T^{(1)} I_1^{(1)}, \tag{11}$$

where $Z_T^{(1)}$ is a transimpedance characterizing cavity 1, loaded by cavity 2 [20],

$$Z_T^{(1)} = \frac{Z_{11}^{(2)} Z_{21}^{(1)}}{Z_{22}^{(1)} + Z_{11}^{(2)}}. \tag{12}$$

Additionally, we can calculate the effective input impedance seen at the input of cavity 1, $V_1^{(1)} = Z_{\rm in}^{(1)} I_1^{(1)}$,

$$Z_{\rm in}^{(1)} = \frac{Z_{11}^{(1)} - \left(Z_{12}^{(1)}\right)}{\left(Z_{22}^{(1)} + Z_{11}^{(2)}\right)}. \tag{13}$$

We now calculate the amount of power entering each cavity. In the case of cavity 1, we have $P_{\rm in}^{(1)} = (1/2){\rm Re}[Z_{\rm in}^{(1)}]|I_1^{(1)}|^2$, and for cavity 2, $P_{\rm in}^{(2)} = (1/2)|V_2^{(1)}|^2{\rm Re}[1/Z_{11}^{(2)}]$. Using the transimpedance, Eq. (11), we have for the ratio of powers,

$$\frac{P_{\rm in}^{(2)}}{P_{\rm in}^{(1)}} = \frac{\left|Z_{21}^{(1)}\right|^2}{\left|Z_{22}^{(1)} + Z_{11}^{(2)}\right|^2} \frac{{\rm Re}\left[Z_{11}^{(2)}\right]}{{\rm Re}\left[Z_{\rm in}^{(1)}\right]}. \tag{14}$$

In principle, we can generate an ensemble of values for the power ratio (14) once we know the radiation impedances of the three ports involved and the quality factors of the two cavities. We combine this information through (1) and (2) with Monte Carlo generated values for the two $\underline{\underline{\xi}}$ matrices and evaluate the matrix elements needed to form (14). Examples of this will be displayed subsequently.

If however, we are in the high-loss limit, we can proceed more directly. Specifically, in the high-loss limit, the diagonal elements of the impedance matrix (1) can be replaced by non-fluctuating radiation impedances for each port, a method also used in fluctuating scattering matrices [21]. The off-diagonal elements of the impedance matrix are small, and according to Eq. (1), can be expressed as a product of a fluctuating quantity $\delta\xi_{12}^{(1)}$ with a simple probability distribution function and the square roots of the two port radiation resistances $Z_{21}^{(1)} = \delta\xi_{21}^{(1)}(R_{11,\rm rad}^{(1)} R_{22,\rm rad}^{(1)})^{1/2}$. Here, the superscript to the variable $\delta\xi_{12}^{(1)}$ indicates that it is drawn from an ensemble representing cavity 1 and has a probability distribution function appropriate to the loss parameter in that cavity. Furthermore, owing to the small value of the off-diagonal elements in the impedance matrices, the input impedance for cavity 1, (13) can be approximated by $Z_{11,\rm rad}^{(1)}$. The result for the transimpedance (12) is

$$Z_T^{(1)} \simeq \frac{Z_{11,\rm rad}^{(2)}}{Z_{22}^{(1)} + Z_{11}^{(2)}} \left(R_{11,\rm rad}^{(1)} R_{22,\rm rad}^{(2)}\right)^{1/2} \delta\xi_{21}^{(1)}, \tag{15}$$

and the result for the power ratio in the high-loss limit can be expressed compactly,

$$\frac{P_{\rm in}^{(2)}}{P_{\rm in}^{(1)}} = \left|\delta\xi_{12}^{(1)}\right|^2 T^{(12)}, \tag{16}$$

where

$$T^{(12)} = \frac{R_{22,\rm rad}^{(1)} R_{11,\rm rad}^{(2)}}{\left|Z_{22,\rm rad}^{(1)} + Z_{11,\rm rad}^{(2)}\right|^2}. \tag{17}$$

Thus, in the high-loss limit, the transmitted power ratio is the product of a statistical quantity characterizing the transmission

of power from port 1 to port 2 in cavity 1, $|\delta\xi_{12}^{(1)}|^2$, and a deterministic quantity describing the transmission of power from port 2 of cavity 1 to port 1 of cavity 2, $T^{(12)}$. We note the maximum value of the transmission coefficient given by Eq. (17) occurs when the two ports have equal radiation resistance, and their radiation reactances cancel ($T_{\max}^{(12)} = 1/4$). Furthermore, according to Eq. (7), $|\delta\xi_{12}|^2$ can be expressed as

$$|\delta\xi_{12}|^2 = (2\pi\alpha^{(1)})^{-1}x, \tag{18}$$

where the probability distribution for the random variable x is universal,

$$f_x(x) = \exp(-x). \tag{19}$$

Using (18) in Eq. (16) shows that the ratio of powers can be expressed as a product of three factors,

$$\frac{P_{\text{in}}^{(2)}}{P_{\text{in}}^{(1)}} = T^{(12)}(2\pi\alpha^{(1)})^{-1}x. \tag{20}$$

One factor x, is statistical, whereas, α describes the losses in the cavity, and $T^{(12)}$ describes the connection between the cavities. This form will be repeated when we consider chains of cavities.

We note that the effect of short transmission delays between the ports can now be included by appropriately modifying the input impedance $Z_{11,\text{rad}}^{(2)}$ to include the transmission line. Specifically, $Z_{11,\text{rad}}^{(2)}$ should be replaced as follows [22]

$$Z_{11,\text{rad}}^{(2)} \to Z_{11,\text{rad}}^{(2)} = Z_0\frac{Z_{11,\text{rad}}^{(2)} + j\ \tan\ \omega\tau Z_0}{Z_0 + j\ \tan\ \omega\tau Z_{11,\text{rad}}^{(2)}},$$

where Z_0 is the characteristic impedance of the transmission line, $\tau = l/\upsilon$ is the delay time, l is the transmission line length, and υ is the phase velocity of the wave traveling inside the transmission line. The above replacement assumes that the statistical fluctuations in the cavity impedance occur on a finer scale in the frequency than the inverse of the delay time. That is, the frequency spacing between modes in the cavity is smaller than τ^{-1}. If the transmission line is so long that this inequality is not satisfied, then the line must be treated as a separate cavity.

We conclude this section with a few examples of our theory. In particular, we illustrate the probability distribution function (PDF) of exact [by exact, we mean using (12) in conjunction with (11)] versus approximate [by approximate, we mean taking the high-loss limit (7)] coupling transimpedance, and the PDF of the coupled power ratio, both in the case of two interconnected cavities. To generate values of the transimpedance and the power ratio using Monte Carlo technique, we first generate elements of the $\underline{\underline{\xi}}$ matrix (3) for each cavity. This is performed by generating a 600×600 random matrix from the GOE and finding its eigenvalues. The eigenvalues are then scaled to have mean separation of unity in the center of the band. We subsequently generate random coupling factors w_{jm} and compute the sum in Eq. (3) with a selected value of the loss parameter α. This procedure is repeated 500 times for each cavity to generate an ensemble of $\underline{\underline{\xi}}$ matrices. Finally, we compute the "dressed" impedance matrix (1) by choosing values for the radiation impedances for the ports. The specific values we chose were $Z_{11,\text{rad}}^{(1)} = Z_{11,\text{rad}}^{(2)} = Z_{11,\text{rad}}^{(3)} = 20 + j50\Omega$.

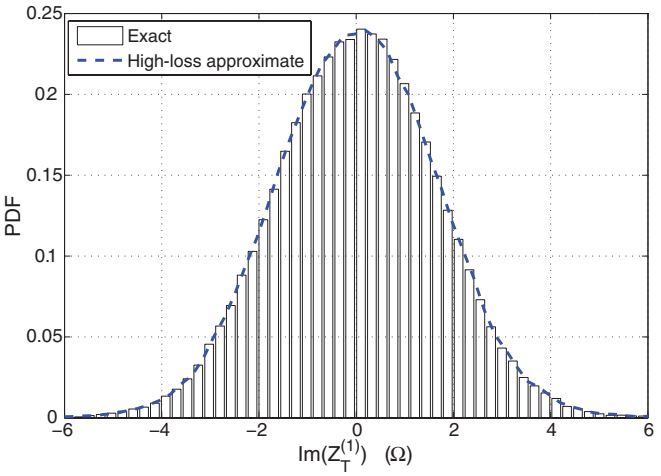

FIG. 2. (Color online) Imaginary part of the coupling impedance for a linear chain of two cavities: Black solid bars: comparison between exact, and blue dashed bars: approximate probability density functions for $\alpha = 6$.

Figure 2 shows the computation of the imaginary part of the coupling impedance $Z_T^{(1)}$ for a linear chain of two cavities with a loss factor of $\alpha = 6$.

In Fig. 2, the dashed line corresponds to the high-loss limit, in which case, we have the approximation (15) where $\delta\xi_{21} = \delta X_{21} + j\delta Y_{21}$, where δX_{21} and δY_{21} are zero mean Gaussian random variables with variance $(2\pi\alpha)^{-1}$. Thus, in this case, the imaginary part of $Z_T^{(1)}$ is predicted to be a zero mean Gaussian random variable with standard deviation 2.3. The solid bars are the result of the Monte Carlo evaluation of (12) without resorting to the high-loss approximation. For this large value of loss parameter, the agreement is quite good.

Figure 3 shows a similar plot for which the loss parameter has been lowered to $\alpha = 1$. In this case, the high-loss approximation deviates from the exact distribution function as calculated by the Monte Carlo method. This deviation becomes more severe as α is lowered. In fact, in the limit $\alpha \to 0$,

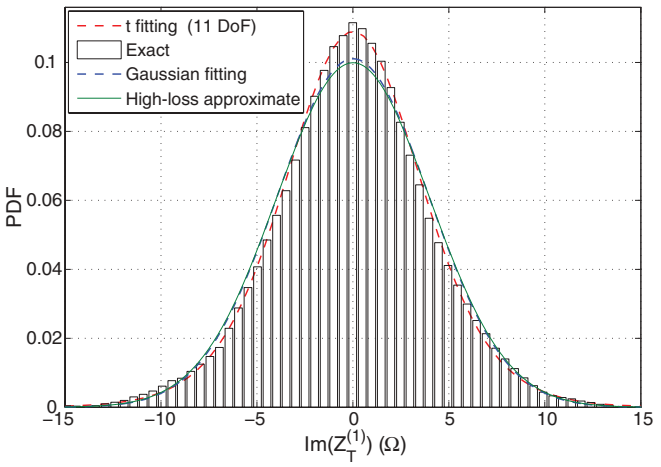

FIG. 3. (Color online) Imaginary part of the coupling impedance for a linear chain of two cavities: Black solid bars: comparison between exact, and blue dashed line: approximate probability density functions for $\alpha = 1$.

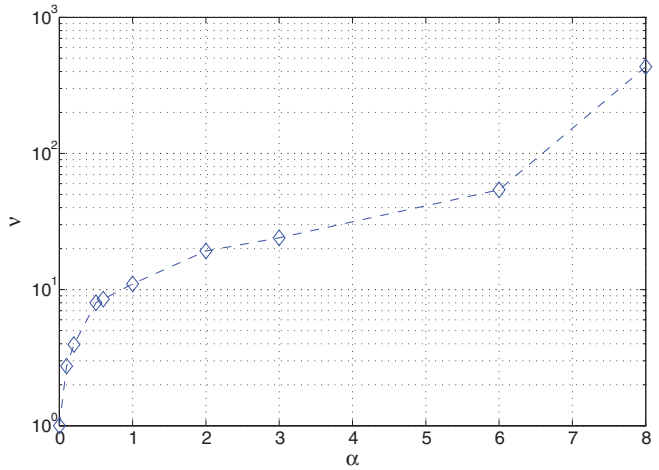

FIG. 4. (Color online) Best-fit determination of the number of degrees of freedom ν of the t distribution modeling the transimpedance of two coupled cavities versus loss parameter α.

the elements of the impedance matrix approach a Lorenzian distribution. For intermediate values of α, there are no simple analytic formulas for the distributions of the elements of the impedance matrix. However, we have investigated the fitting of the transimpedance to the t distribution with ν degrees of freedom,

$$f_t(t) = \frac{\Gamma[(\nu+1)/2]}{\sqrt{\nu\pi}\,\Gamma(\nu/2)}\left(1+\frac{t^2}{\nu}\right)^{-(\nu+1)/2},$$

where Γ is the Γ function, and which also reproduces the transition from Lorenzian at $\nu = 1$ to Gaussian as $\nu \to \infty$. Also shown in Fig. 3 are the best-fit Gaussian and the best-fit t distribution with $\nu \approx 11$. The t distribution better matches the Monte Carlo results. The Kolmogorov-Smirnov test confirms the departure for the Gaussian profile: The null hypothesis of *equal distributions* is rejected with a maximum distance statistic $D_{\max} = 0.0235$, greater than the critical value $CV_\beta = 0.0157$ with a significance level $\beta = 0.05$. Repeating the same analysis with profiles of Fig. 2 yields the expected outcome

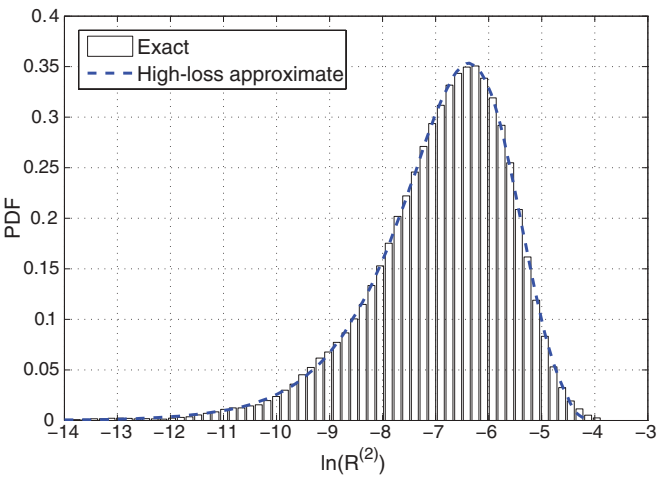

FIG. 5. (Color online) Power ratio for a linear chain of two cavities: Black solid bars: comparison between exact and blue dashed line: approximate probability density functions for $\alpha = 6$.

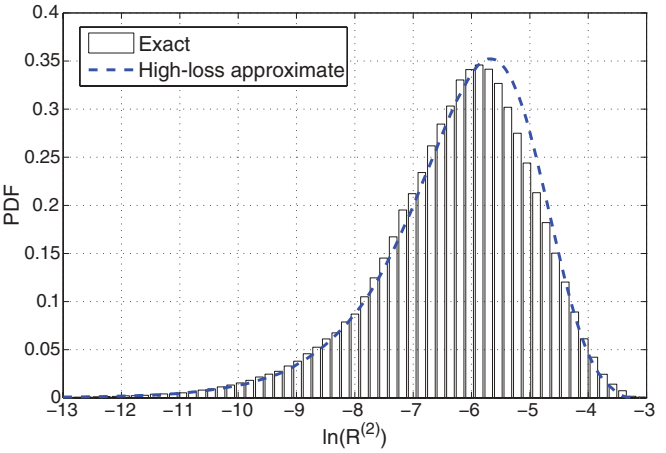

FIG. 6. (Color online) Power ratio for a linear chain of two cavities: Black solid bars: comparison between exact and blue dashed line: approximate probability density functions for $\alpha = 3$.

$D_{\max} < CV_{0.05}$, where $D_{\max} = 0.0053$ indicates accepting the null hypothesis. Fitting the transimpedance to t distributions for other values of the loss parameter α results in the behavior of ν with α in the transition between the lossless and the high-loss cases as shown in Fig. 4.

Figures 5–7 show the power ratio (14) for the same cases as Figs. 2 and 3 and with $\alpha = 6, 3$, and 1, respectively. Here, it can be seen that the case $\alpha = 6$ is well represented by the high-loss limit, whereas, for the case $\alpha = 1$, significant discrepancies appear, and the full Monte Carlo evaluation is necessary.

III. COUPLING IN A CHAIN OF CAVITIES

We now analyze linear chains of arbitrary length as depicted in Fig. 1. In this situation, the nth cavity in the chain with $n \geqslant 2$ is excited by the field leaking from the $(n-1)$-th cavity, and it excites the $(n+1)$-th cavity in the same way. We can use the formulas for the two-cavity case to provide an iterative solution to the N-cavity chain problem. For example, using (13), we can calculate the input impedance for the nth cavity in the chain in terms of the elements of the nth impedance

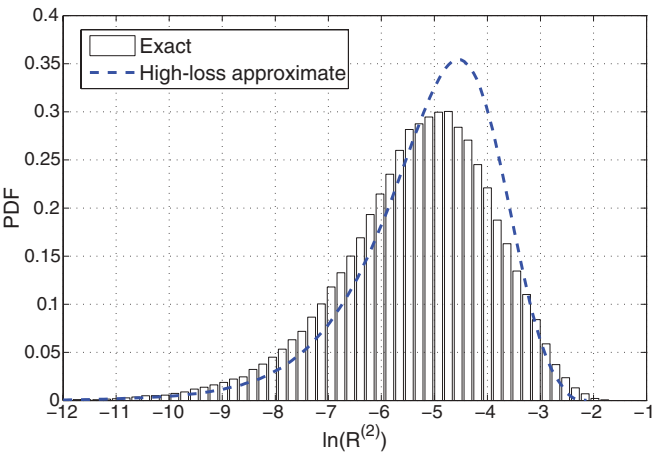

FIG. 7. (Color online) Power ratio for a linear chain of two cavities: Black solid bars: comparison between exact and blue dashed line: approximate probability density functions for $\alpha = 1$.

matrix and the input impedance of the $(n+1)$-th cavity,

$$Z_{\rm in}^{(n)} = \frac{Z_{11}^{(n)} - \left(Z_{12}^{(n)}\right)^2}{\left(Z_{22}^{(n)} + Z_{\rm in}^{(n+1)}\right)}. \tag{21}$$

This expression can be iterated starting at the last cavity where $Z_{\rm in}^{(N)} = Z_{11}^{(N)}$ to the first cavity to find $Z_{\rm in}^{(1)}$.

The transimpedance for the nth cavity relates the voltage at the input of the $(n+1)$-th cavity to the current at the input of the nth cavity. This can be calculated by generalizing (13),

$$Z_T^{(n)} \equiv \frac{V_1^{(n+1)}}{I_1^n} = \frac{Z_{\rm in}^{(n+1)} Z_{21}^{(n)}}{Z_{22}^{(n)} + Z_{\rm in}^{(n+1)}}. \tag{22}$$

From Eq. (22), we can find the ratio of the input voltage at the $(n+1)$-th cavity for the input voltage at the nth cavity,

$$\frac{V_1^{(n+1)}}{V_1^n} = \frac{Z_T^{(n)}}{Z_{\rm in}^{(n)}} = \frac{Z_{\rm in}^{(n+1)} Z_{21}^{(n)}}{Z_{\rm in}^{(n)}\left(Z_{22}^{(n)} + Z_{\rm in}^{(n+1)}\right)}. \tag{23}$$

From Eq. (23), we also compute the ratio of power coupled into the $(n+1)$-th cavity to that coupled into the nth cavity,

$$\rho^{(n)} \equiv \frac{P_{\rm in}^{(n+1)}}{P_{\rm in}^{(n)}} = \frac{\left|Z_{21}^{(n)}\right|^2}{\left|Z_{22}^{(n)} + Z_{\rm in}^{(n+1)}\right|^2} \frac{{\rm Re}\left[Z_{\rm in}^{(n+1)}\right]}{{\rm Re}\left[Z_{\rm in}^{(n)}\right]}. \tag{24}$$

Thus, the ratio of power entering the Nth cavity to that entering the first cavity can be expressed as a product,

$$R^{(N)} \equiv \frac{P_{\rm in}^{(N)}}{P_{\rm in}^{(1)}} = \prod_{n=1}^{N-1} \rho^{(n)}. \tag{25}$$

The case of high loss and correspondingly weak fluctuations, described by Eqs. (6) and (7), leads to an expression for the coupled power ratio $R^{(N)}$ that factorizes

$$\frac{P_{\rm in}^{(N)}}{P_{\rm in}^{(1)}} = X^{(N)} \prod_{n=1}^{N-1} \frac{T^{(n,n+1)}}{2\pi\alpha^{(n)}}, \tag{26}$$

where fluctuations are described by the random variable $X^{(N)}$,

$$X^{(N)} \equiv \prod_{n=1}^{N-1} x^{(n)}, \tag{27}$$

which is a product of $N-1$ independent and identically distributed random variables [23,24] with distribution given by Eq. (18). The transmission factors follow from (16),

$$T^{(n,n+1)} = \frac{R_{22,\rm rad}^{(n)} R_{11,\rm rad}^{(n+1)}}{\left|Z_{22,\rm rad}^{(n)} + Z_{11,\rm rad}^{(n+1)}\right|^2}, \tag{28}$$

describing the coupling between the nth and the $(n+1)$-th cavity, and the loss factor,

$$\alpha^{(n)} = \frac{k^2}{(Q^{(n)}\Delta k^{2,(n)})} \tag{29}$$

describes the ratio of the Q width to the spacing between modes in the nth cavity.

The ensemble average of Eq. (23) is easily derived as

$$\left\langle \frac{P_{\rm in}^{(N)}}{P_{\rm in}^{(1)}} \right\rangle = \prod_{n=1}^{N-1} \frac{T^{(n,n+1)}}{2\pi\alpha^{(n)}}, \tag{30}$$

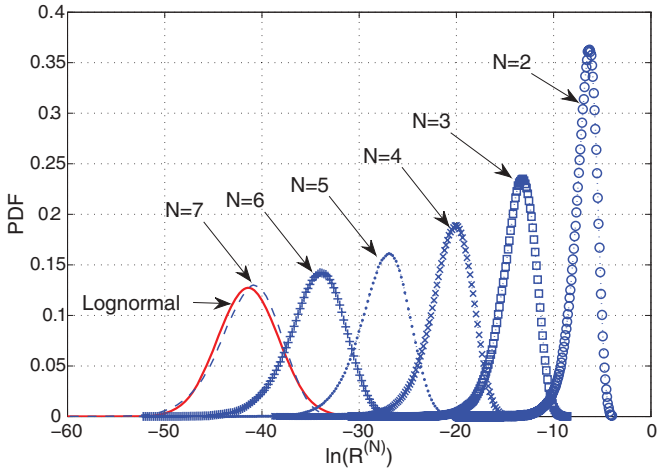

FIG. 8. (Color online) Probability density function of power ratios for chains of up to seven cavities: the transition between an exponential $n=2$ and a lognormal distribution becomes evident at $N \simeq 7$ in the high-loss limit $\alpha = 6$.

depending only on properties of ports and average distributed losses of each cavity. To derive (30), we have used $\langle X^{(N)} \rangle = 1$.

We now use the Monte Carlo method to generate ensembles of impedance matrices and to compute the coupling in chains of cavities. We basically generate the impedance matrices for each single cavity and combine them using the theoretical expressions (21) and (22) according to the method described in Sec. II. We then evaluate the power ratio for sequences of cavity chains of different lengths. For these studies, the cavities were assumed to be *statistically identical* with port radiation impedances $Z_{11,\rm rad}^{(n)} = Z_{22,\rm rad}^{(n)} = (20 + j50)\,\Omega$. The PDFs of the logarithm of the power ratio for the case $\alpha = 6$ is shown in Fig. 8 and, for $\alpha = 1$, is shown in Fig. 9. The high-loss case (Fig. 8) is well approximated by the analytic formulas (26) and (27). These are not shown but would be indistinguishable from the Monte Carlo results. Also, the distribution approaches

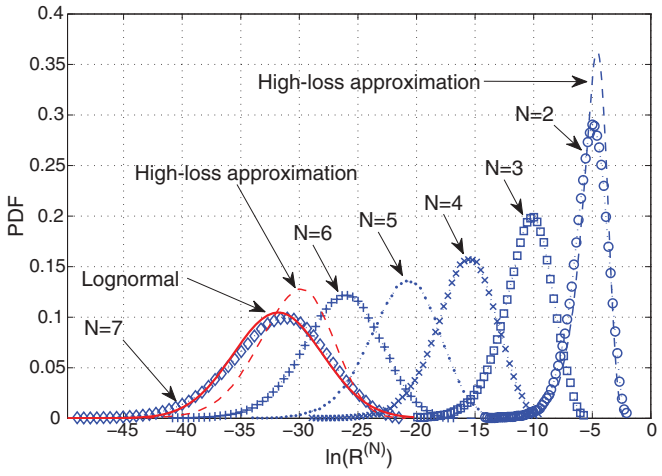

FIG. 9. (Color online) Probability density function of exact power ratios for chains of up to seven cavities with $\alpha = 1$. For a large number of cavities, the distribution approaches solid red line: a lognormal with a mean variance that differs from the high-loss prediction.

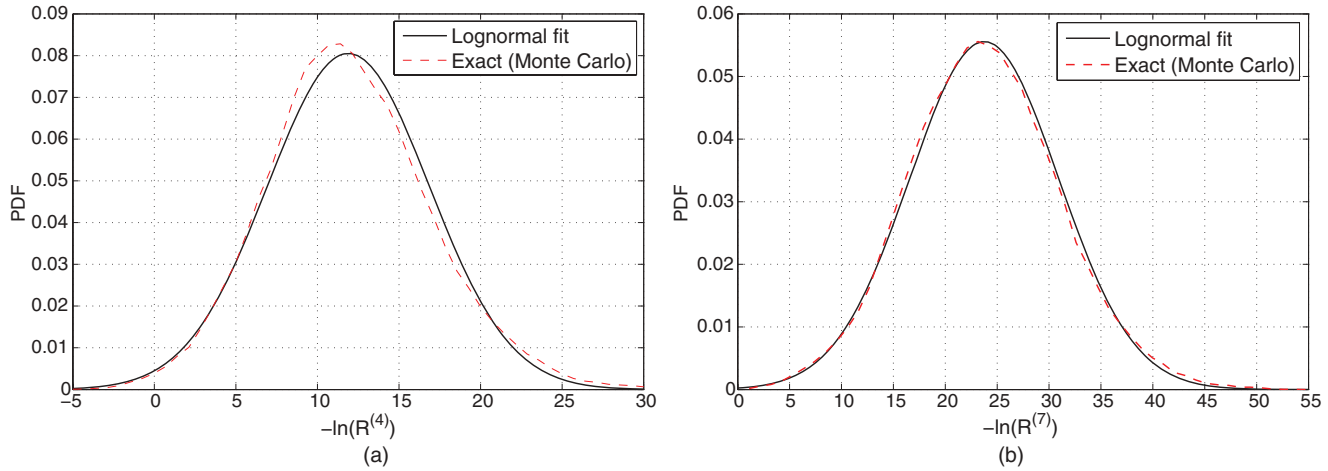

FIG. 10. (Color online) Probability density function of exact power ratios for lossless chains ($\alpha = 0$) with (a) $N = 4$ cavities and (b) $N = 7$ cavities. In the lossless case, the convergence to a lognormal distribution is rapid. The distributions have variances equal to twice the mean.

lognormal as the number of cavities becomes large. This is evident from the comparison of the seven-cavity chain with a best-fit *lognormal* distribution. This behavior is expected since, according to Eqs. (26) and (27), the power ratio becomes a product of N independent and identically distributed random variables, and thus, as N becomes large, the logarithm of the power ratio is normally distributed.

In the low-loss case ($\alpha = 1$, Fig. 9), the distribution of power ratios for a chain with only a few cavities deviates from the high-loss predictions (as also seen in Fig. 3). Here, we have shown, as dashed (blue $N = 2$, red $N = 7$) lines, the high-loss predictions. However, as the number of cavities in the chain increases, the asymptotic distribution again approaches *lognormal* but with a different mean and variance than in the high-loss case.

The distribution functions for the power ratio in the lossless ($\alpha = 0$) case are shown in Fig. 10 for $N = 4$ and $N = 7$ cavities. It is again seen that, as the number of cavities N becomes large, the distribution functions approach lognormal. However, in this case, the approach to lognormal appears to be much more rapid. The lognormal distribution with an exponential decrease in the power ratio as the cavity number is increased is a signature of Anderson localization.

We note that it is not surprising that the power ratio approaches a lognormal distribution as the number of cavities increases as this is common behavior in systems in which random matrices are multiplied. A prime example is that of Anderson localization in a one-dimensional lattice. It has already been shown that the Anderson localization occurs in a chain of random impedances [25]. In our case, the interconnected elements are cavities.

The 2×2 impedance matrix $Z_{\rm pl}^{(n)}$ [Eq. (8) for cavity n] relates the pair $V_1^{(n)}$ and $V_1^{(n+1)} = V_2^{(n)}$ to $I_1^{(n)}$ and $I_1^{(n+1)} = -I_2^{(n)}$. The relation between voltages and currents can be rearranged such that

$$\begin{pmatrix} V_1^{(n)} \\ I_1^{(n)} \end{pmatrix} = \underline{\underline{M}}^{(n)} \begin{pmatrix} V_1^{(n+1)} \\ I_1^{(n+1)} \end{pmatrix}, \tag{31}$$

where $M_{11}^{(n)} = Z_{11}^{(n)}/Z_{12}^{(n)}$, $M_{21}^{(n)} = (Z_{12}^{(n)})^{-1}$, $M_{12}^{(n)} = [Z_{11}^{(n)} Z_{22}^{(n)} - (Z_{21}^{(n)})]/Z_{12}^{(n)}$, and $M_{22}^{(n)} = Z_{22}^{(n)}/Z_{12}^{(n)}$. With $M_{\rm pl}^{(n)}$, we denote the pth row lth column element of the transfer matrix $\underline{\underline{M}}^{(n)}$ between cavity n and cavity $n+1$. We also note that $\det[\underline{\underline{M}}^{(n)}] = 1$.

Thus, the input voltage and current at cavity 1 can be expressed in terms of a product of matrices and the voltage and current in the load ($V_1^{(n+1)} = Z_L I_1^{(n+1)}$),

$$\begin{pmatrix} V_1^{(1)} \\ I_1^{(1)} \end{pmatrix} = \prod_{n=1}^{N} \underline{\underline{M}}^{(n)} \begin{pmatrix} V_1^{(n+1)} \\ I_1^{(n+1)} \end{pmatrix}. \tag{32}$$

The matrices $\underline{\underline{M}}^{(n)}$ are independent and are identically distributed, thus, for almost any value of Z_L, the ratio of the voltage and current at the input to that at the load grows exponentially with N. This situation is analogous to the Lyapunov exponent of a chaotic nonlinear system [26]. In particular, one expects the largest eigenvalue λ_N of the product matrix $\prod_{n=1}^{N} \underline{\underline{M}}^{(n)}$ to behave as

$$\lambda_N \simeq \exp(Nh), \tag{33}$$

where h, the finite N Lyapunov exponent, has a characteristic probability density function $P(h)$ [26],

$$P(h) = \left(\frac{2\pi}{NG''(h)}\right)^{1/2} \exp[-NG(h)]. \tag{34}$$

Here, $G(h)$ is a positive function that has a minimum value $G(\bar{h}) = 0$, where $\bar{h}$ is the corresponding Lyapunov exponent. In Eq. (34), $G''(h) \triangleq d^2G(h)/dh^2$. Thus, Taylor expanding $G(h)$ about $\bar{h}$, one observes that $P(h)$ is approximated by a normal distribution. We note that, since $\det[\underline{\underline{M}}^{(n)}] = 1$, the smallest eigenvalue is given by $\lambda_N^{(s)} \simeq \exp(-Nh)$, and it describes the reciprocal case where power is injected in the last cavity and is extracted from the first one.

To test Eq. (34), we extract $G(h)$ from the data for $f_R(\ln R^{(N)})$ plotted in Figs. 8–10.

Specifically, we consider the histograms $f_R(\ln R^{(N)})$ for each value of α and N. We then define $h = -\ln R^{(N)}/N$, and

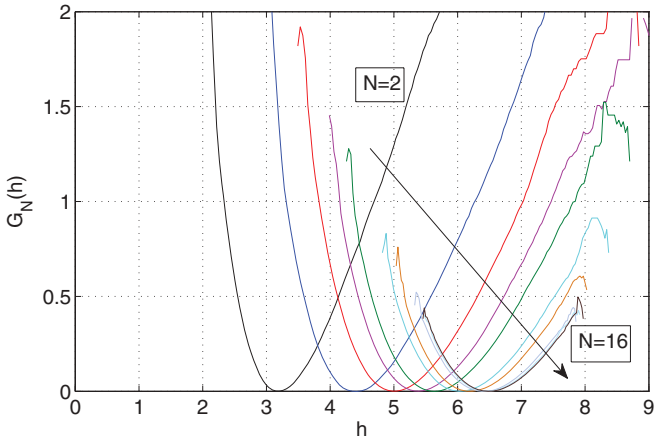

FIG. 11. (Color online) The quantity $G_N(h)$ [Eq. (35)] in the high-loss case ($\alpha = 6$) with increasing N. $G_N(h)$ approaches an asymptotic limit as $N \to \infty$. However, the approach is relatively slow.

for each value of h, we compute

$$G_N(h) = \frac{1}{N}\{\ln(f_{R^{(N)},\max}) - \ln[f_{R^{(N)}}(\ln\ R_N)]\}, \qquad (35)$$

where $f_{R^{(N)},\max}$ is the maximum value of the histogram for the given values of α and N. If Eq. (34) holds, then $G_N(h)$ should become independent of N as N increases. The results of this procedure are shown in Fig. 11 for $\alpha = 6$ and in Fig. 12 for $\alpha = 0$. We note that, in both cases, as N increases, G_N takes on the expected parabolic shape. The convergence to an asymptotic function is slower in the $\alpha = 6$ case than in the $\alpha = 0$ case.

IV. STRUCTURE IMPEDANCE

We explore the convergence of the power ratio to lognormal by considering the dependence of the localization rate on the cavity number. Specifically, we define an effective localization rate to be the value of $\bar{h}_N$ in Eq. (35) that gives $G_N(\bar{h}_N) = 0$ for a chain of N cavities.

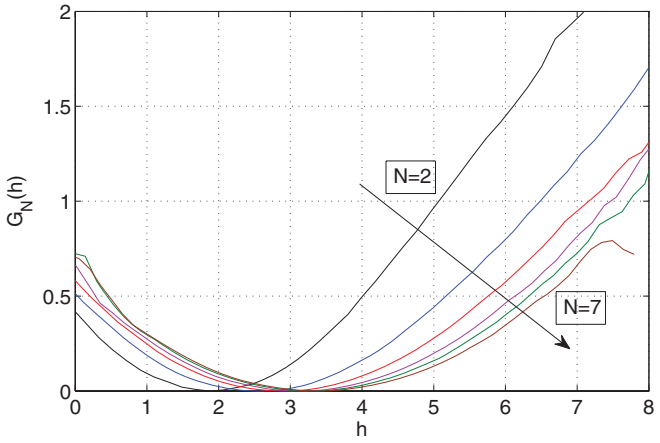

FIG. 12. (Color online) The quantity $G_N(h)$ in the lossless case ($\alpha = 0$) with increasing N. The function approaches an asymptotic value more quickly than in the $\alpha = 6$ case.

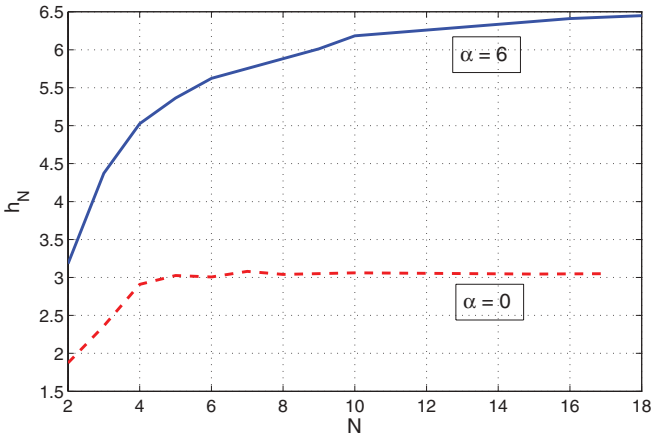

FIG. 13. (Color online) The quantity $\bar{h}_N$ in high loss $\alpha = 6$ and lossless $\alpha = 0$ cases with increasing N. Its physical meaning is the inverse of the localization length.

Equivalently, this is the value $h_N = -\ln(R_N)/N$ for which $f_R(\ln\ R^{(N)})$ is maximum. We plot $\bar{h}_N$ versus N in Fig. 13 for the case of $\alpha = 6$ and $\alpha = 0$.

We again see that convergence to an asymptotic value as predicted by Eq. (34) is faster in the $\alpha = 0$ case than in the $\alpha = 6$ case.

Finally, we note that Eq. (34) predicts the expectation in the limit $N \to \infty$,

$$E[(h - \bar{h})^2] = \frac{1}{NG''(\bar{h})},$$

where $\bar{h} = \bar{h}_{N\to\infty}$ and $(\cdot)''$ again stands for the second-order derivative with respect to h.

This implies that, in the limit $N \to \infty$,

$$\mathrm{Var}\,[\ln\ R_N] = \gamma\, E\,[\ln\ R_N]\,,$$

where $\gamma = [\bar{h}G''(\bar{h})]^{-1}$. The numeral values of γ that we found are $\gamma(\alpha = 0) \simeq 2$ and $\gamma(\alpha = 6) \simeq 0.2$. The factor of 2 in Eq. (38), between variance and mean value of a lognormal fluctuation, surprisingly represents the same result predicted by the Dorokhov-Mello-Pereyra-Kumar equation for the conductance of finite-length quantum wires (see Fig. 19 and comments therein of Ref. [27]) and is confirmed by numerical computations of the Anderson model. This similarity can be explained by noting that the conductance of small chunks of quantum wires, connected by short leads, is expressed as the product of transmission coefficients according to the Landauer formula [28,29].

V. CONCLUSION

We have investigated the statistical aspects of coupling in a chain of electromagnetic cavities. Our main assumptions are that the coupling from one cavity to the next occurs through a set of ports that support a single mode of propagation and that the behavior of fields within each cavity is described by the random coupling model. Generally, the first assumption requires that the transverse dimensions of the ports be smaller

than a wavelength. The second assumption requires that the cavity be much larger than a wavelength. In the model, each cavity is described by a loss parameter α given by Eq. (5). When this loss parameter is greater than unity interference at the input port of a cavity due to waves reflected at the output port of the same cavity, it can be neglected. However, interference due to waves propagating through multiple paths from input to output is retained in the random coupling. This case, which we refer to as the high-loss case, leads to a general formula [Eq. (26)] for the coupled power, given by the product of transmission factors describing the coupling between cavities, factors describing the loss in each cavity, and products of universal random variables. When the loss parameter is unity or smaller than a Monte Carlo simulation, evaluation of the power fluctuations is required. In both high- and low-loss cases, the power coupled into the last cavity of a long chain slowly tends to a lognormally distribution. Finally, if the chain is made of lossless cavities, we find rapid convergence to the lognormal distribution. The present paper develops and extends previous results obtained for RCM [30–32].

ACKNOWLEDGMENTS

We wish to acknowledge the helpful comments of the Maryland Wave Chaos Group. This work was supported by AFOSR Grant No. FA95501010106 and ONR Grant No. N000140911190.

[1] M. Wright and R. Weaver, *New Directions in Linear Acoustics and Vibration: Quantum Chaos, Random Matrix Theory and Complexity* (Cambridge University Press, Cambridge, UK, 2010).
[2] P. A. Mello and N. Kumar, *Quantum Transport in Mesoscopic Systems: Complexity and Statistical Fluctuations* (Oxford University Press, Oxford, 2010).
[3] G. E. Mitchell, A. Richter, and H. A. Weidenmuller, Rev. Mod. Phys. **82**, 2845 (2010).
[4] D. A. Hill, *Electromagnetic Fields in Cavities: Deterministic and Statistical Theories* (Wiley, Hoboken, NJ, 2009).
[5] F. Haake, *Quantum Signature of Chaos* (Springer, Berlin, 2010).
[6] H.-J. Stockmann, *Quantum Chaos* (Cambridge University Press, Cambridge, UK, 1999).
[7] M. L. Mehta, *Random Matrices* (Elsevier, Amsterdam, 2004).
[8] P. A. Mello, P. Peveyra, and T. H. Seligman, Ann. Phys. **161**, 254 (1985).
[9] P. W. Brouwer, Phys. Rev. B **51**, 16878 (1995).
[10] E. Doron, U. Smilansky, and T. Dittrich, Physica B **179**, 1 (1992).
[11] K. Takahashi and T. Aono, Phys. Rev. E **75**, 026207 (2007).
[12] G. B. Tait, R. E. Richardson, M. B. Slocum, M. O. Hatfield, and M. J. Rodriguez, IEEE Trans. Electromagn. Compat. **53**, 229 (2011).
[13] G. B. Tait, R. E. Richardson, M. B. Slocum, M. O. Hatfield, and M. J. Rodriguez, IEEE Trans. Electromagn. Compat. **53**, 846 (2011).
[14] X. Zheng, T. M. Antonsen, and E. Ott, Electromagnetics **26**, 3 (2006).
[15] X. Zheng, T. M. Antonsen, and E. Ott, Electromagnetics **26**, 33 (2006).
[16] S. Hemmady, X. Zheng, T. M. Antonsen, E. Ott, and S. M. Anlage, Phys. Rev. Lett. **94**, 014102 (2005).
[17] S. Hemmady, X. Zheng, T. M. Antonsen, E. Ott, and S. M. Anlage, Phys. Rev. E **71**, 056215 (2005).
[18] J. A. Hart, T. M. Antonsen, and E. Ott, Phys. Rev. E **80**, 041109 (2009).
[19] J.-H. Yeh, J. A. Hart, E. Bradshaw, T. M. Antonsen, E. Ott, and S. M. Anlage, Phys. Rev. E **82**, 041114 (2010).
[20] N. Balabanian and T. A. Bickart, *Electrical Network Theory* (Wiley, New York, 1969).
[21] B. Dietz, T. Friedrich, H. L. Harney, M. Miski-Oglu, A. Richter, F. Schafer, and H. A. Weidenmuller, Phys. Rev. E **81**, 036205 (2010).
[22] S. Ramo, J. R. Whinnery, and T. Van Duzer, *Fields and Waves in Communication Electronics* (Wiley, New York, 1994).
[23] A. Papoulis, *Probability, Random Variables, and Stochastic Processes* (McGraw-Hill, New York, 1991).
[24] J. Galambos and I. Simonelli, *Products of Random Variables* (Dekker, New York, 2004).
[25] E. Akkermans and R. Maynard, J. Phys. (Paris) **45**, 1549 (1984).
[26] P. Grassberger, R. Badii, and A. Politi, J. Stat. Phys. **51**, 8 (1988); T. Horita, H. Hata, and H. Mori, Prog. Theor. Phys. **83**, 1065 (1990); A. Crisanti, G. Paladin, and A. Vulpiani, *Products of Random Matrices in Statistical Physics* (Springer, Berlin, 1993).
[27] C. W. J. Beenakker, Rev. Mod. Phys. **69**, 3 (1997).
[28] Y. V. Fyodorov and H.-J. Sommers, J. Math. Phys. **38**, 1918 (1997).
[29] J. J. M. Verbaarschot, H. A. Weidenmueller, and M. R. Zirnbauer, Phys. Rep. **129**, 367 (1985).
[30] S. Hemmady, X. Zheng, J. Hart, X. Zheng, T. M. Antonsen, E. Ott, and S. M. Anlage, Phys. Rev. E **74**, 036213 (2006).
[31] X. Zheng, S. Hemmady, T. M. Antonsen, S. M. Anlage, and E. Ott, Phys. Rev. E **73**, 046208 (2006).
[32] L. M. Pecora, H. Lee, D.-H. Wu, T. M. Antonsen, M.-J. Lee, and E. Ott, Phys. Rev. E **83**, 065201(R) (2011).